Optical properties of coevaporated $AgSiO_x$ cermet films

David Evans*
Physics Department, Victoria University of Wellington, Private Bag, Wellington, New Zealand
(Received 28 December 1984)

Measurements have been made of the optical properties of coevaporated $AgSiO_x$ cermet films. Films varying in metal fraction from 0% to 100% were prepared in a residual oxygen atmosphere, and at slow evaporation rates, to give oxygen-rich films. Measurements of reflectance and transmittance were inverted to give the complex dielectric constant by an iterative method using a Kramers-Kronig integral of the transmittance. The results are compared with the Maxwell-Garnett and Sheng effective-medium theories for spherical particles. A previously unreported peak in the imaginary part of the dielectric constant was observed for high-volume-fraction cermets. A number of films were examined with a transmission electron microscope.

I. INTRODUCTION

Recently there has been interest in the optical properties of cermets with the intention of creating materials with desirable absorptance and emittance for solar-energy collection applications.[1,2] The optical measurements made on a cermet are frequently analyzed by determining an effective dielectric constant ($\epsilon=\epsilon_1+i\epsilon_2$) for the medium. The aim of most researchers in this field has been to find an effective-medium theory (EMT) that predicts the effective dielectric constant of a cermet from the dielectric constants and volume-fractions of the components. A number of EMT's have been proposed and it has been found that the best theory for a particular cermet depends on the cermet microstructure. There are two primary classes of microstructure, the first is the isolated grain structure where grains of one component are entirely surrounded by the other component, and the second is the aggregate structure where both components are randomly distributed. The Maxwell-Garnett[3] theory is applicable to the isolated grain structure and the Bruggeman[4] theory to the aggregate structure.[5]

The optical properties of noble-metal cermets have been studied for some time[6–9] and the comparisons with theory have been made with respect to the transmittance or absorptance. However more insight into the relationships between microstructure and optical properties can be obtained by calculating the effective dielectric constant for the cermets as has been done for $AuAl_2O_3$,[10,5,11] $AuMgF_2$,[12,10] and AuMgO.[10,13,5]

In order to most clearly compare real composite media with the predictions of EMT's, components with simple optical properties were selected. The components chosen were Ag and SiO_x with the optical measurements being made in the visible region of the spectrum. Silver was chosen for its relative inertness and its similarity in this region to an ideal free-electron metal. The insulator was required to be transparent over as wide a wavelength range as possible and SiO_x, after uv exposure (see below), fulfilled this need. The optical measurements made on each cermet were carefully analyzed to give an effective dielectric constant for the composite. The microstructure was found to be most like the isolated grain structure, and the results will be compared with a simplified variant of the Sheng EMT (Refs. 14—16, and 11) which is closely related to the Maxwell-Garnett (MG) theory. It was found that for low-volume-fraction cermets the simplified Sheng theory gave a good representation of the major features of the measured effective dielectric constants.

In the next section the preparation and characterization of the cermets is discussed, and in Sec. III the method used to give the effective dielectric constant from the optical measurements is described. Section IV gives a brief presentation of the EMT's used in Sec. V which covers the comparison of the experimental data with theory. The origin of a previously unreported peak in the imaginary part of the dielectric constant for high metal-volume-fraction cermets is also discussed in Sec. V.

II. EXPERIMENTAL

The cermets were prepared by coevaporation onto fused silica substrates in a stainless-steel vacuum chamber evacuated by a 150 mm diffusion pump with a liquid-nitrogen cold trap. The room-temperature substrate was mounted on the lid of the chamber and on either side are two water-cooled quartz-crystal microbalances. Below the substrate are the resistively heated evaporation boats and between them is a shield so that each microbalance crystal can "see" only one boat. At the base of the chamber there is a leak valve which can be used to regulate the pressure in the evaporation system.

The cermets were evaporated with the pressure in the chamber at 5×10^{-6} Torr because it is known that the SiO will getter oxygen as it is deposited, resulting in an oxygen rich SiO_x film. It has been found[17] that this procedure followed by exposure of the film to strong uv light causes the absorption edge of the SiO_x to move further into the uv. In the case of the SiO_x deposited for this work the edge moved to above 5.5 eV and there was virtually no absorption in the experimentally measured region. The cermets were exposed to a 100 W mercury vapor lamp for 8 h this exposure time was chosen after observing the resistance of some of the cermets during the treatment.

The resistance approached a limiting value exponentially with a time constant of 1 to 3 h, and by the end of an 8-h exposure the resistance had stabilized. The samples were at a distance of 8 cm from the uv source.

The cermets were prepared with the aid of a microcomputer-based deposition-rate monitor described elsewhere.[18] The rate is determined by measuring the period of the microbalance crystals which have one face exposed to the evaporant vapor stream. The period of the oscillation varies with the mass deposited on the crystal, and by determining the average period over equally spaced time intervals the microcomputer calculates the rate from the difference between successive intervals. The total mass deposited during an evaporation can also be determined by the microcomputer. The microcomputer acts as a feedback system which holds the deposition rate constant by controlling the power delivered to the evaporation boats. The uniformity of the evaporation rate depends on the rate required, the worst case variation being $\pm 10\%$ and of a short duration. It is unlikely that the composition of the cermets varied significantly over their thickness.

The period change of the microbalances was calibrated against film thickness by depositing pure films of each cermet component, and measuring their thickness by an independent method. Once this was done the microbalance measurements for a cermet deposition could be used to estimate the metal-volume-fraction. While this method gives accurate mass fractions, unfortunately it does not necessarily give a true volume-fraction as it is likely that there are voids present in the cermet.[9] Some measurements of the cermet resistivity were made and the metal-insulator transition occurred at approximately 47% silver. Considering all sources of error the relative uncertainty in the cermet volume-fractions determined in this way is about $\pm 6\%$.

A number of cermets were deposited onto thin carbon or colloidion films mounted on copper electron-microscope grids, and examined with a Phillips EM420 transmission electron microscope (TEM). These cermets were deposited at the same pressure as the cermets for optical measurements. The silver was found to be in the form of rounded islands varying in size from the resolution limit of the microscope up to a few hundred nanometers in diameter. The most important observation made was that the cermets had an islandlike structure for all volume-fractions. As the metal fraction was increased the insulator was found as a coating on the metal islands, and beyond the percolation threshold it must be contained in irregularly shaped regions between the islands, but not preventing metal-metal contact.

Photographs were taken of the electron diffraction pattern of the silver islands and the average silver crystallite size was estimated from the breadth of the diffraction rings.[19] The average island sizes did not vary greatly with volume-fraction, being less than 5 nm up to 75% silver. This indicates that although the films had some large islands they represented a small fraction of the total silver, and/or were comprised of small crystallites. The latter is probable since thin twins were visible in some of the larger islands.

Reflectance (R) and transmittance (T) of the samples were measured by the differential technique suggested by Beaglehole,[20] using a system constructed at Victoria University by Staines.[21] The wavelength range covered was 220 to 800 nm. For the measurement of R a freshly deposited (<2 h old) aluminum film was used as a reference. The uncertainty in T was approximately ± 0.01, but for R the uncertainty may be slightly larger due to the use of literature values[22] for the reflectance of the aluminum reference.

III. EVALUATION OF ϵ FROM R AND T

In order to make the most fundamental comparison of theoretical predictions with experimental data the complex dielectric constant was calculated from the optical measurements. It is assumed that the films may be described by a homogeneous effective dielectric constant, but it should be appreciated that this may not be valid for very thin films, or for films with inhomogeneities of the scale of the wavelength. The most common method of determining ϵ is to minimize the difference between the experimental R and T and that calculated using the Fresnel equations,[23] by an iterative technique starting from an approximate value for ϵ.[24,25] This method has been used by many researchers but was found to be unsatisfactory for the cermets described here, due to the existence of multiple solutions, or no solutions at all, in some wavelength regions. For this reason a method similar to that described by Bringans[26] was used.

Following the method proposed by Nilsson[24] the dielectric constant was determined using the Kramers-Kronig integral relating the absolute value and phase shift of the complex transmittance. It was assumed that the transmittance was constant above and below the experimental range, and the contribution to the phase shift from these regions was determined by specifying the total phase shift at two wavelengths within the experimental range. These phase shifts were obtained from initial estimates of the dielectric constant found by the R and T iterative technique. Once the phase shift was known the dielectric constant could be calculated, and in turn the reflectance of a film with this dielectric constant and thickness. The best estimate of the dielectric constant for the cermet was found by minimizing the difference between the calculated and experimental reflectances, with the specified phase shifts and film thickness as variables.

The major source of error in this process is due to the assumption that the transmittance of the cermets is constant outside the experimental region. Near the limits of the experimental wavelength range the real part of the dielectric constant was very sensitive to the specified phase shift. To demonstrate the consequences of changing the specified phase shift values Fig. 1 gives the dielectric constant for a 25% cermet. The figure shows the best-fit dielectric constant determined as described above, and also the dielectric constant when one of the specified phase shifts has been changed by $\pm 10°$. This was sufficient to give a sum of squares for the difference between the calculated and experimental R that was at least four times the optimum value. Although these solutions are

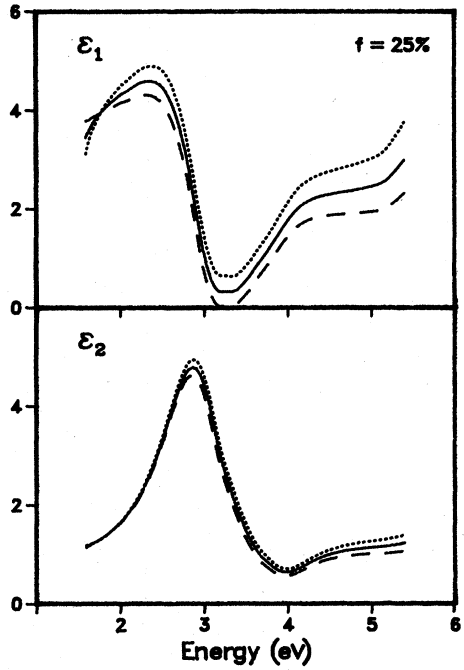

FIG. 1. Effect of changing one of the specified phase shifts by ±10°. The solid curve gives the best fit to the experimental reflectance.

well removed from the best fit the ϵ_2 curves are only changed in magnitude and not shape. The same is true for ϵ_1 except at low energies where changes in shape occur.

For films containing more than 75% silver the assumption that the transmittance is constant at low energies is particularly poor. For these films it was assumed that the transmittance varied as $(\hbar\omega)^2$, which is typical of a free-electron metal, in order to calculate the contribution to the phase shift from the low-energy region.

The important points concerning uncertainties in the dielectric constants are:

(1) The position of features in ϵ_1 and ϵ_2 is determined accurately.

(2) The shape of features will be correct provided they are not near the extremities of the curves.

(3) The shape of the ϵ_1 curve at low energies may be incorrect.

(4) There are uncertainties in the magnitudes of the curves with ϵ_2 being known most accurately.

IV. EFFECTIVE-MEDIUM THEORIES

It is generally agreed that the Maxwell-Garnett theory is the most appropriate EMT for cermets with the isolated grain structure typical of $AgSiO_x$ cermets. This is especially true for low-volume-fraction $AgSiO_x$ cermets in the visible region, where the optical properties are dominated by a resonance in the dielectric constant often called the dielectric anomaly, which is not predicted by the Bruggeman theory.

In practice there are two MG equations, they are:

$$\epsilon=\epsilon_i\frac{\epsilon_m+2\epsilon_i+2f(\epsilon_m-\epsilon_i)}{\epsilon_m+2\epsilon_i-f(\epsilon_m-\epsilon_i)}\,, \tag{1}$$

$$\epsilon=\epsilon_m\frac{\epsilon_i+2\epsilon_m+2(1-f)(\epsilon_i-\epsilon_m)}{\epsilon_i+2\epsilon_m-(1-f)(\epsilon_i-\epsilon_m)}\,, \tag{2}$$

where ϵ_m and ϵ_i are the dielectric constants of the metal and insulator, respectively, and f is the metal-volume-fraction. The first equation is for metal islands embedded in an insulator host and the second is for the reverse topology. In the case of cermets where their behavior changes smoothly with volume-fraction from insulating to metallic we might expect Eq. (1) to be applicable at low-volume-fractions and (2) at high-volume-fractions. However they do not describe a continuous solution for the effective dielectric constant, as for no filling fraction (other than $f=1$ or $f=0$) do they give the same result.

Recently an EMT has been proposed by Sheng[14–16] that combines features of both MG equations and gives a dielectric constant that varies continuously from insulating to metallic, and predicts a percolation threshold. The Sheng (S) theory was originally derived for spheroids but the simpler form for spheres[11] will be used here; the equation is

$$\frac{3P}{2+\frac{\epsilon_a}{\epsilon}}+\frac{3(1-P)}{2+\frac{\epsilon_b}{\epsilon}}=1\,, \tag{3}$$

where ϵ_a is given by Eq. (1) and ϵ_b by Eq. (2). The factor P is determined by the volume-fraction and is given by

$$P=\frac{(1-f^{1/3})^3}{(1-f^{1/3})^3+[1-(1-f)^{1/3}]^3}\,. \tag{4}$$

When f is less than 0.2, $P\simeq 1$, and the simplified S equation gives almost identical results to the first MG equation; similarly when f is greater than 0.8 the dielectric constant is almost identical to that given by the second MG equation.

V. COMPARISON OF DATA WITH THEORY

Figures 2 and 3 give the real and imaginary parts (ϵ_1 and ϵ_2, respectively) of the dielectric constant for a selection of films. For the pure SiO_x film ϵ_1 is almost constant for all energies and ϵ_2 is so small that it is not discernible on the figure. For the 8% cermet ϵ_1 is very similar but the presence of the silver has increased ϵ_2, and a very broad peak centered near 3.3 eV is just visible. This peak is due to the dielectric anomaly and it is well defined in the 16% and 34% cermets; the shift of the dielectric anomaly to lower energies as the volume-fraction is increased is evident. Structure due to the anomaly is also visible in ϵ_1 for these two cermets. It should be recalled from Sec. III that the ϵ_1 values are least reliable at the ends of the curves, so the curves have been truncated to include only that data which are believed to be close to the real value. This restriction is only severe for very low-volume-fractions, and for most cermets the data is good from 2 to 5 eV. The curves for ϵ_2 are better behaved as they are more closely related to a directly measured quan-

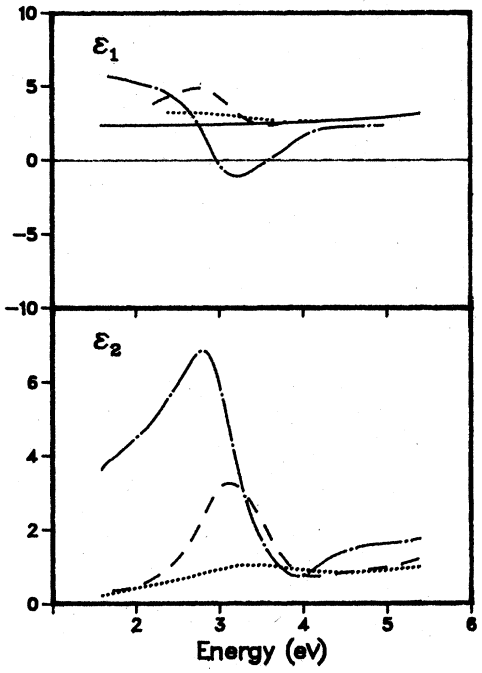

FIG. 2. Experimental dielectric constant for four films. Solid line, pure SiO_x; dotted line, 8% silver; dashed line, 16% silver; chain-dotted line, 34% silver.

tity (the absorptance of the sample) and have not been truncated.

For the 73% cermet, and for pure silver, ϵ_1 is large and negative at low energies, as would be expected for a free-electron metal film. The imaginary part of the dielectric constant shows a corresponding increase. There is a shoulder on the low-energy ϵ_2 of the 73% cermet that suggests an underlying peak, and also a slight peak in ϵ_2 of the pure silver film near 3.5 eV; the interpretation of these peaks will be discussed later in this section. At energies above 4 eV there is an increase in ϵ_2 due to interband absorption in the silver. This is of course most pronounced for the pure silver film.

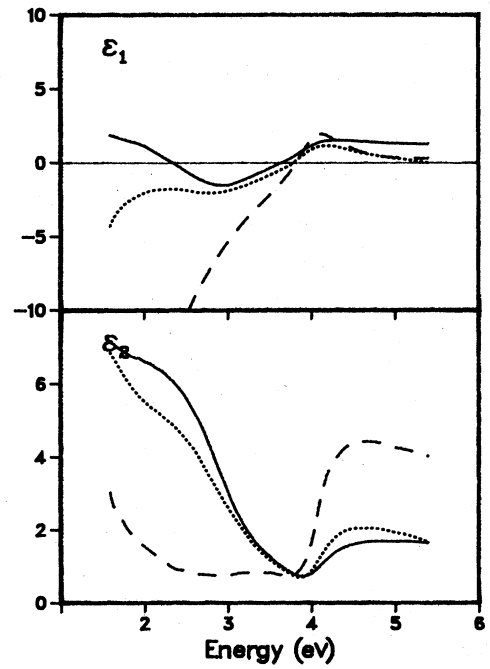

FIG. 3. Experimental dielectric constant for three films. Solid line, 58% silver; dotted line, 73% silver; dashed line, pure silver.

A. Model dielectric constants for cermet components

The EMT's introduced in Sec. IV provide a method for calculating an effective dielectric constant for a composite from the dielectric constants of the components and their volume fractions. The experimentally determined values of the dielectric constant for pure SiO_x and pure Ag could have been used for ϵ_i and ϵ_m, but due to uncertainties in the measured values the use of model parameters seemed more appropriate. Although these models may be an oversimplication they will not introduce features in the effective dielectric constant that are not a result of the EMT. A model for ϵ_i can be devised without departing markedly from the measured dielectric constant of SiO_x. The real part of ϵ_i was chosen to be constant ($\epsilon_1=2.25$), and the imaginary part zero, across the entire experimental range. This is a good approximation as can be seen in Fig. 2.

For ϵ_m it was assumed that the dielectric constant of pure Ag is made up of a Drude free-electron part, and a part due to interband transitions. To find the appropriate Drude parameters [the plasma frequency (ω_p) and the relaxation time (τ)] the low-energy part of ϵ for pure Ag was fitted with the Drude expression

$$\epsilon=1-\frac{\omega_p^2}{\omega(\omega+i/\tau)} . \tag{5}$$

The values obtained were $\hbar\omega_p=9.7\pm0.2$ eV and $\hbar/\tau=0.13\pm0.01$ eV ($\tau=4.4\pm0.3$ fs). Once the plasma frequency and relaxation time were known the contribution to the pure silver dielectric constant given by Eq. (5) could be subtracted, and the result is shown as the solid curve in Fig. 4. This is the contribution to the dielectric constant due to interband transitions. The curve for $\epsilon_{2\text{ib}}$ (ib denotes interband) so obtained was modeled by two straight line portions, and by a $1/\hbar\omega$ form at high energies. The real part ($\epsilon_{1\text{ib}}$) was calculated by taking the Kramers-Kronig integral of the $\epsilon_{2\text{ib}}$ model, the result is shown in Fig. 4.

The Drude relaxation time is usually taken to be related to the mean-free-path (l) for electrons in the film by

$$\frac{1}{\tau}=\frac{1}{\tau_0}+\frac{v_F}{l} , \tag{6}$$

where τ_0 is the relaxation time in the bulk metal and v_F is the Fermi velocity. For cermet films it is expected that τ is related to the diameter of the silver particles, or the crystallite size if the particles are not monocrystalline. In the following discussion it will be helpful to adjust ϵ_m to account for a short mean-free-path in the metal particles, and to obtain optimum agreement between experiment

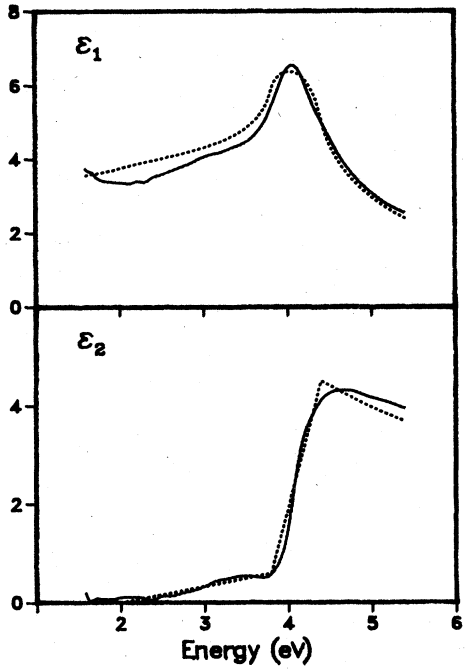

FIG. 4. Interband dielectric constant for pure silver. Solid line, experiment; dotted line, model.

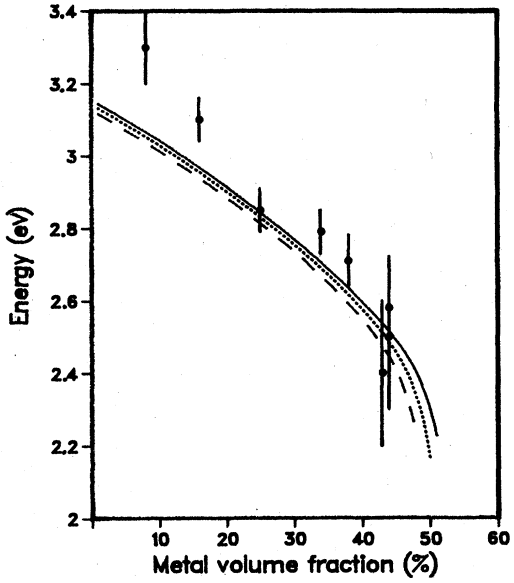

FIG. 5. Position of dielectric anomaly given by simplified S theory and experimental data. Solid line $\hbar/\tau=0.7$ eV; dotted line, $\hbar/\tau=0.9$ eV; dashed line $\hbar/\tau=1.1$ eV.

and theory. To do this a free-electron dielectric constant given by Eq. (5) will be added to the interband dielectric constant shown in Fig. 4. In every case $\hbar\omega_p$ will be as for pure silver (9.7 eV) and $\hbar/\tau$ will be an adjustable parameter with the assumption that Eq. (6) gives an approximate relationship between τ and the mean-free-path.

B. Low-volume-fraction cermets

As the dielectric anomaly is the most important feature of the dielectric constant for low-volume-fraction cermets it is appropriate to base the comparisons between theory and experiment on predictions concerning the anomaly. The most convenient way of doing this is to examine the way the position and shape of the anomaly varies with volume-fraction and relaxation time. It was hoped that this would suggest suitable values of $\hbar/\tau$ to be used for comparison of the experimental data with the EMT's over the entire experimental range. Using the models for ϵ_i and ϵ_m described above, and the simplified S theory, the position, height, and width at half maximum of the dielectric anomaly peak in ϵ_2 were determined as a function of volume-fraction and $\hbar/\tau$. These quantities are plotted in Figs. 5–7 as well as the experimental data. Note that the first MG equation would give identical curves at volume-fractions less than 20%.

The curves for position and height end where the dielectric anomaly changes from being a peak in ϵ_2 to become a shoulder on a Drudelike effective dielectric constant. The width curves end when there is no longer a half-height point on the low-energy side of the peak. Figure 5 shows that the peak moves to lower energies as the volume-fraction increases, and the peak position is only weakly dependent on $\hbar/\tau$. The peak height (Fig. 6) increases as more silver is added, but begins to decrease before it disappears. The peak width (Fig. 7) varies linearly with $\hbar/\tau$ but is almost independent of volume-fraction.

For the two lowest-volume-fraction cermets the peak is at a higher energy than that predicted by the theory. This is contrary to the observation of Liebsch and Gonzalez[27] that experiment usually gives a peak at a lower energy than the MG equation. This is surprising since the MG equation should work best at low-volume-fractions, where the particles are widely spaced. However the size of the

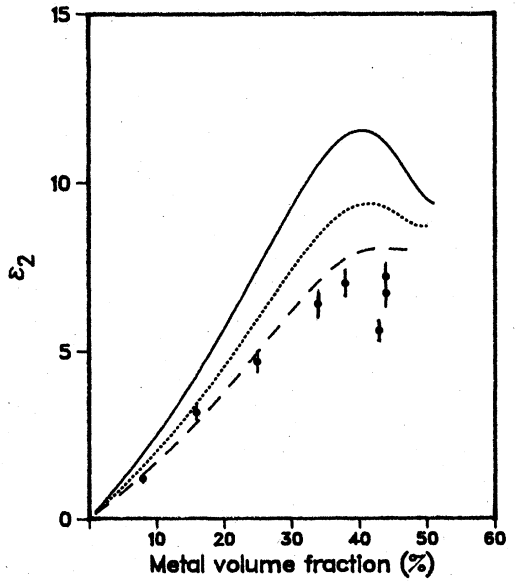

FIG. 6. Height of dielectric anomaly peak in ϵ_2 given by simplified S theory and experimental data. Solid line, $\hbar/\tau=0.7$ eV; dotted line, $\hbar/\tau=0.9$ eV; dashed line $\hbar/\tau=1.1$ eV.

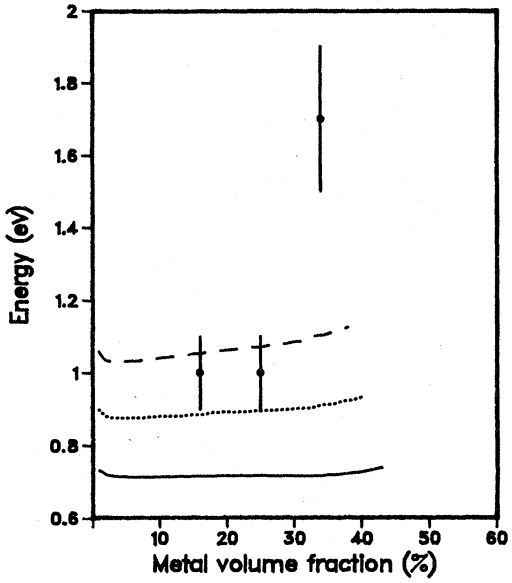

FIG. 7. Width of dielectric anomaly peak in ϵ_2 given by simplified S theory and experimental data. Solid line, $\hbar/\tau=0.7$ eV; dotted line, $\hbar/\tau=0.9$ eV; dashed line $\hbar/\tau=1.1$ eV.

particles is expected to be extremely small, and the use of a bulk metal dielectric constant for ϵ_m may be inappropriate.

The height of the peaks in ϵ_2 follow the curve for $\hbar/\tau=1.1$ eV quite well but the results for the higher-volume-fraction cermets suggest a larger $\hbar/\tau$. Since the silver particles should not be getting smaller at these volume-fractions an increasing $\hbar/\tau$ seems unreasonable. The peak width could only be measured for three cermets, as shown in Fig. 7. The two lower-volume-fraction cermets suggest a value of $\hbar/\tau$ near 1 eV but for the third cermet a higher value is indicated. The large increase in the breadth for this cermet is due to the peak becoming asymmetric, which is not predicted by the MG or S theories.

To provide a qualitative comparison between the experimental dielectric constants and those derived from the simplified S theory Figs. 8 and 9 give the results for two representative cermets. As seen above $\hbar/\tau=1.1$ eV should give a satisfactory fit to the peak shape, and the theoretical curves have been calculated with this value which corresponds to a mean-free-path of 0.8 nm. Although this seems very short in comparison with the observed particle sizes, other researchers[5] have had to use similar values to obtain satisfactory agreement with experiment. Further comment on the choice of $\hbar/\tau$ will be made below. The experimental curves for ϵ differ in magnitude from the theory but have a similar shape, except at the low- and high-energy extremities. The most interesting differences between the experimental and predicted dielectric constants are the asymmetric shape of the peak in ϵ_2 for the 34% cermet, and the incorrect prediction of the peak position for the low-volume-fraction cermets.

The most serious omission from the S theory for predicting the optical properties of cermet films is the interaction between metal particles. The model used for the

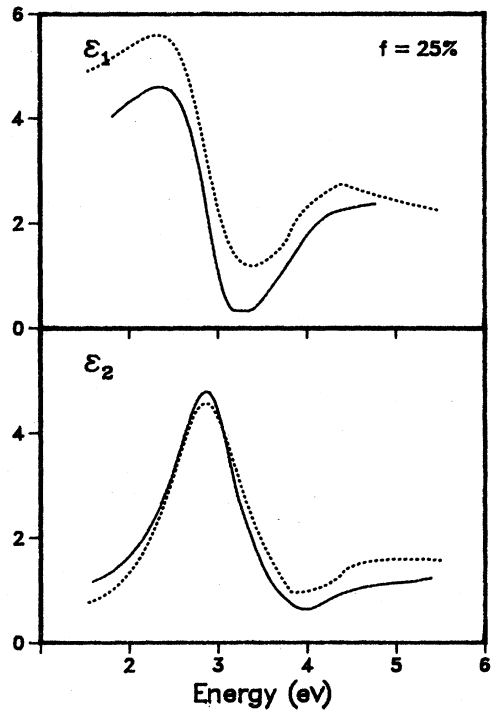

FIG. 8. Experimental dielectric constant for a 25% cermet (solid line), and the dielectric constant given by the simplified S theory with $\hbar/\tau=1.1$ eV (dotted line).

cermet structure is spherical particles placed in a radiation field that is undisturbed by other particles, and so does not allow for the multipoles excited in one particle by the others. The MG equation does allow for the interaction

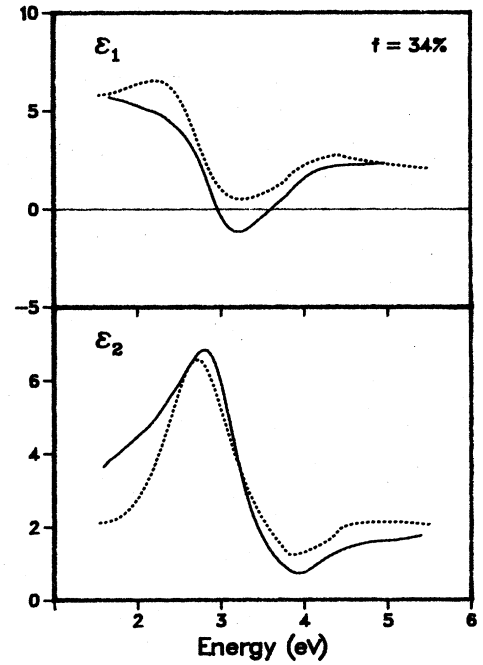

FIG. 9. Experimental dielectric constant for a 34% cermet (solid line), and the dielectric constant given by the simplified S theory with $\hbar/\tau=1.1$ eV (dotted line).

between dipoles on the particles in a cermet, but not in a realistic way. The assumption made is that the particles occupy the sites of a cubic lattice and so does not include the fields due to randomly distributed particles.

A number of methods have been proposed[28,29,27] for determining the effect of randomly placed interacting particles on the effective dielectric constant. There is general agreement that the main effect will be broadening of the dielectric anomaly, and extension of the peak in ϵ_2 to lower energies due to multipole resonances;[28] this may explain the asymmetric peak in Fig. 9. If some of the dielectric anomaly broadening is caused by these effects then the appropriate value for $\hbar/\tau$ would be smaller, and more in keeping with the observed particle sizes. At low volume-fractions (large interparticle spacing) the multipole interactions are not so important,[27] but the peaks are still broadened by disorder in the particle placement. Some authors[27,30] also propose that the anomaly will be shifted to lower energies, but the dielectric anomaly of the two lowest-volume-fraction cermets described here is at a higher energy than that predicted by the theory.

C. High-volume-fraction cermets

The agreement between the experimental results and the simplified S theory for volume-fractions above 50% is not as good as it is below 50%. The results for two representative cermets are given in Figs. 10 and 11. The value of $\hbar/\tau$ was varied to get the best fit for each cermet. The most outstanding difference is the presence of a peak in ϵ_2 (marked E) that is not predicted by the simplified S theory. This peak is at about 2.7 eV in Fig. 10, and moves to about 3.3 eV for the 90% cermet; it cannot be identified with the dielectric anomaly as that peak moves to lower energies with increasing volume-fraction.

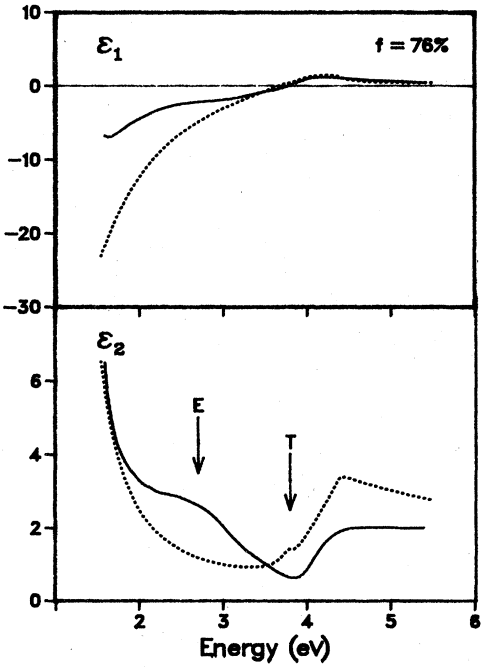

FIG. 10. Experimental dielectric constant for a 76% cermet (solid line), and the dielectric constant given by the simplified S theory with $\hbar/\tau=0.3$ eV (dotted line). The peaks indicated by the arrows are discussed in the text.

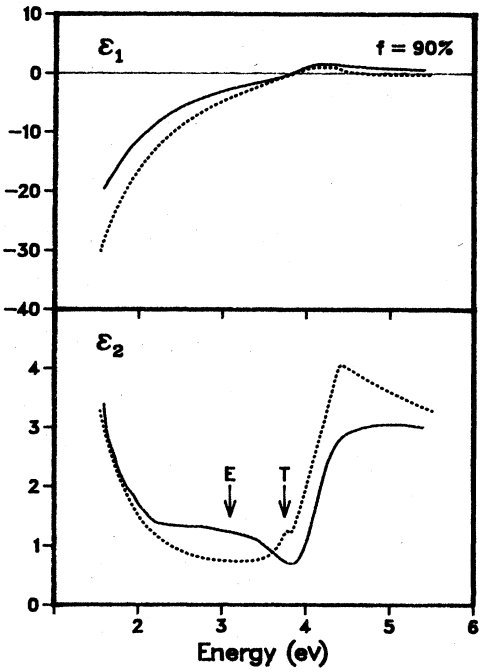

FIG. 11. Experimental dielectric constant for a 90% cermet (solid line), and the dielectric constant given by the simplified S theory with $\hbar/\tau=0.15$ eV (dotted line). The peaks indicated by the arrows are discussed in the text.

There is a small peak in the simplified S theory just below the interband edge which is visible in Figs. 10 and 11 (marked T). This peak is also given by the second MG equation and is the analog of the dielectric anomaly in the first MG equation; i.e., it is a feature due to insulator islands surrounded by metal. The peak is broadened by an increase in $\hbar/\tau$ but is never as large as the dielectric anomaly peak, and it moves to slightly higher energies as the volume-fraction decreases. Consequently it seems unreasonable to identify the E peak observed in the cermet ϵ_2 with the T peak in the simplified S and MG theories. However these theories were derived for spherical insulator particles in a metal host, which is not the case for the cermets being discussed. As observed in Sec. II even at high-volume-fractions the metal is in the form of islands, and presumably the insulator is in the form of strands between the islands. A more realistic model for the shape of the insulator particles would be narrow cylinders or prolate spheroids.

The MG theory has been extended[31,32] to spheroidal particles with one axis perpendicular to the surface of the medium, but with the other axes in random directions. The S theory was also derived for spheroidal particles but in the high-volume-fraction limit should give a similar result to the simpler MG equation. Plotted in Fig. 12 is the effective dielectric constant of an 80% cermet calculated using the models of Sec. V A for spherical particles, and prolate spheroidal particles with one of the minor axes

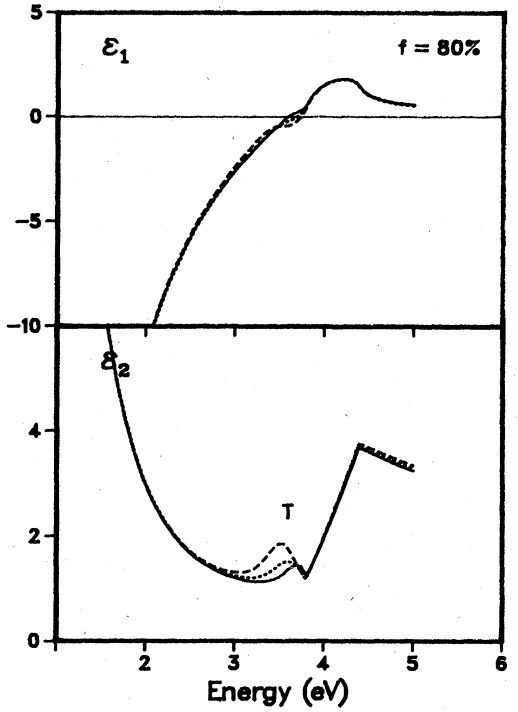

FIG. 12. Dielectric constant given by the MG theory for an 80% cermet. Solid line, spherical particles; dotted line, eccentricity (e)=0.9; dashed line, e=0.99.

perpendicular to the surface of the cermet. The curves for two values of the eccentricity are given. An eccentricity of 0.9 corresponds to a major:minor axis ratio of 3.2:1, and e=0.99 corresponds to 10:1. From the figure it can be seen that increasing the eccentricity increases the size of the T peak and moves it to lower energies. It is not possible, however, to move the peak far enough to agree with the experimental curves of Figs. 10 and 11 as increasing the eccentricity beyond 0.99 has little additional effect on the position of the peak. The MG theory as used in this section is for particles that are much smaller than the wavelength of the radiation, but it is possible that as the eccentricity of the spheroids is increased and their length approaches λ, the inclusion of multipole effects could move the T peak to even lower energies.

Another possible explanation for the E peak in ϵ_2 is that the excitation of surface plasmons on the surface of the cermet is causing additional absorption of the incident radiation. The surface plasmon frequency (ω_s) for a boundary between a metallic medium and a dielectric[33] is determined by the condition

$$\epsilon_1 = -\epsilon_d \ , \tag{7}$$

where the real part of the dielectric constant of the metallic medium is ϵ_1 and the dielectric constant of the dielectric is ϵ_d. Surface plasmon absorption was observed for silver/air interfaces by Jasperson and Schnatterly[34] at a photon energy of about 3.5 eV, and it seems likely that the small peak just below 3.5 eV for the pure silver film (Fig. 4) is due to surface plasmons. If this peak corresponds to $\hbar\omega_s$ then it might be expected that $\epsilon_1=-1$ at this energy, but from the experimental data presented here it was found to be -2 ± 1. Jasperson and Schnatterly found that the peak occurred at an energy where ϵ_1 was between -1 and -2, and attributed the shift to surface contamination. There is however reason for expecting a peak due to surface plasmons to be at an energy less than $\hbar\omega_s$ even with no surface contamination, as will be explained.

For a smooth surface a photon has insufficient momentum to couple to the surface plasmon modes, but surface roughness may provide the required k_r to excite a surface plasmon. The surface plasmon may then emit a photon in a nonspecular direction and the film will appear to have an increased absorption. The energy spectrum of the surface plasmons excited depends upon the k_r vectors that are present in the surface roughness, but obviously only photons with $\omega \lesssim \omega_s$ can couple to the surface plasmons. Thus $\hbar\omega_s$ given by Eq. (7) would be an upper limit on a surface plasmon peak in ϵ_2, and not necessarily the center.

For all cermet films exhibiting the unexplained peak the value for ϵ_1 was found to be -2.0 ± 0.5 at the energy where the center of the peak occurred. This is strong evidence for the proposition that the E peak in ϵ_2 is associated with surface plasmon absorption. If this is the case then there is no evidence in the experimental data of the T peak, which is surprising since as indicated above the peak is expected to be larger for a real cermet than for the theoretical models treated by the EMT's. Further experimental work on the nonspecular reflectance of cermets may be of assistance in determining the cause of the observed peak.

Priestley *et al.*[9] have reported observing surface plasmons in thin $AgSiO_2$ cermet films. They made measurements with an angle of incidence of 60° to the film normal and found an absorption peak for p polarized light. This peak was at about 3.8 eV for pure silver films and moved down in energy as the metal-volume-fraction was decreased. This absorption mode was first observed for thin pure silver films[35] and occurs at the plasma energy. The excitation of the surface plasmons results from the coupling between electromagnetic waves on the two film surfaces. This mode does not rely on surface roughness to be excited and is distinct from the surface plasmon absorption discussed above. Such a mode was not observed in the work described here because as measurements were made at normal incidence there was no electric field component perpendicular to the film. However the measured plasma energies of the cermets prepared for this work do compare favorably with the data given by Priestly *et al.*

VI. CONCLUSION

A study has been made of the optical properties of $AgSiO_x$ cermets covering a wide composition range. The transmittance and reflectance of the cermets were analyzed to give the effective dielectric constant for the films, and this was compared with the predictions of two EMT's. It was found that the simplified Sheng theory

gave results that were close to the experimental data for cermets containing less than 50 volume percent metal.

For cermets containing more than 50 volume percent metal the agreement was not satisfactory. This was partly due to the presence of a peak in the experimental data for the imaginary part of the dielectric constant, that is not predicted by the EMT's. Two possible sources of this peak were identified.

ACKNOWLEDGMENT

The author wishes to thank Professor D. Beaglehole for many helpful suggestions.

---

*Present address: Division of Information Technology, Department of Scientific and Industrial Research, Private Bag, Lower Hutt, New Zealand.

[1]J. I. Gittleman, B. Abeles, P. Zanzucchi, and Y. Arie, Thin Solid Films **45**, 9 (1977).

[2]G. A. Niklasson and C. G. Granqvist, J. Appl. Phys. **55**, 3382 (1984).

[3]J. C. Maxwell-Garnett, Philos. Trans. R. Soc. London **203**, 385 (1904).

[4]D. A. G. Bruggeman, Ann. Phys. (Liepzig) **24**, 636 (1935).

[5]U. J. Gibson, H. G. Craighead, and R. A. Buhrman, Phys. Rev. B **25**, 1449 (1982).

[6]R. H. Doremus, J. Chem. Phys. **40**, 2389 (1964).

[7]R. H. Doremus, J. Chem. Phys. **42**, 414 (1965).

[8]R. W. Cohen, G. D. Cody, M. D. Coutts, and B. Abeles, Phys. Rev. B **8**, 3689 (1973).

[9]E. B. Priestley, B. Abeles, and R. W. Cohen, Phys. Rev. B **12**, 2121 (1975).

[10]C. G. Granqvist, J. Appl. Phys. **50**, 2916 (1979).

[11]U. J. Gibson and R. A. Buhrman, Phys. Rev. B **27**, 5046 (1983).

[12]P. H. Lissberger and R. G. Nelson, Thin Solid Films **21**, 159 (1974).

[13]S. Berthier and J. Lafait, Thin Solid Films **89**, 213 (1982).

[14]P. Sheng, Phys. Rev. Lett. **45**, 60 (1980).

[15]P. Sheng, Phys. Rev. B **22**, 6364 (1980).

[16]P. Sheng, in *Lecture Notes in Physics No. 154,* edited by R. Burridge, S. Childress, and G. Papanicolaou (Springer, Berlin, 1982).

[17]A. P. Bradford, G. Hass, M. McFarland, and E. Ritter, Appl. Opt. **4**, 971 (1965).

[18]D. Evans, B. Hall, and J. E. Morris, J. Phys. E **16**, 544 (1981).

[19]H. P. Klug and L. E. Alexander, *X-ray Diffraction Procedures for Polycrystalline and Amorphous Materials* (Wiley, New York, 1974).

[20]D. Beaglehole, Appl. Opt. **7**, 2218 (1968).

[21]M. P. Staines, Ph.D. thesis, Victoria University of Wellington, 1979 (unpublished).

[22]*A.I.P. Handbook* (McGraw-Hill, New York, 1972), p. 6—157.

[23]O. S. Heavens, *Optical Properties of Thin Solid Films* (Butterworth, London, 1950).

[24]P. O. Nilsson, Appl. Opt. **7**, 435 (1968).

[25]F. Abeles and M. L. Theye, Surf. Sci. **5**, 325 (1966).

[26]R. D. Bringans, J. Phys. D **10**, 1855 (1977).

[27]A. Liebsch and P. V. Gonzalez, Phys. Rev. B **29**, 6907 (1984).

[28]D. R. McKenzie and R. C. McPhedran, in *Electrical Transport and Optical Properties of Inhomogeneous Media (Ohio State University, 1977),* proceedings of the First Conference on the Electrical Transport and Optical Properties of Inhomogeneous Media, edited by J. C. Garland and D. B. Tanner (AIP, New York, 1978), p. 283; W. T. Perrins, R. C. McPhedran, and D. R. McKenzie, Thin Solid Films **57**, 321 (1979).

[29]W. Lamb, D. M. Wood, and N. W. Ashcroft, Phys. Rev. B **21**, 2248 (1980).

[30]W. T. Doyle, in *Electrical Transport and Optical Properties of Inhomogeneous Media (Ohio State University, 1977),* Proceedings of the First Conference on The Electrical Transport and Optical Properties of Inhomogeneous Media, edited by J. C. Garland and D. B. Tanner (AIP, New York, 1978), p. 300.

[31]O. Hunderi, Phys. Rev. B **7**, 3419 (1973).

[32]C. G. Granqvist, in *Electrical Transport and Optical Properties of Inhomogeneous Media (Ohio University 1977),* proceedings of the First Conference on the Electrical Transport and Optical Properties of Inhomogeneous Media, edited by J. C. Garland and D. B. Tanner (AIP, New York, 1978), p. 196.

[33]E. A. Stern and R. A. Ferrell, Phys. Rev. **120**, 130 (1960).

[34]S. N. Jasperson and S. E. Schnatterly, Phys. Rev. **188**, 759 (1969).

[35]A. J. McAlister and E. A. Stern, Phys. Rev. **132**, 1599 (1963).